Work Summary

Advancing the tight-binding model by considering two spin half electrons hopping on 4 sites. Also considered the possibility of having two cavities and two qubits in simulation.

Main Work

0. Comments on the control dynamics results
1. Further verification for variational method
2. Tight-binding model generalization
3. Tight-binding model: 2 spin-half electrons on 4 sites
4. Control with double cavity

Comments on the control dynamics results

Figure 1 is an example plot of observable fluctuation under GRAPE optimized control. After reading some materials and consulting some people, I think the spikes at the end of pulse sequences are understandable since they may occur from interference between phases. I have also tried to input smoothed optimized pulse sequences into the GRAPE algorithm, but I don't think GRAPE supports that function for now. That might be implemented with some further work.

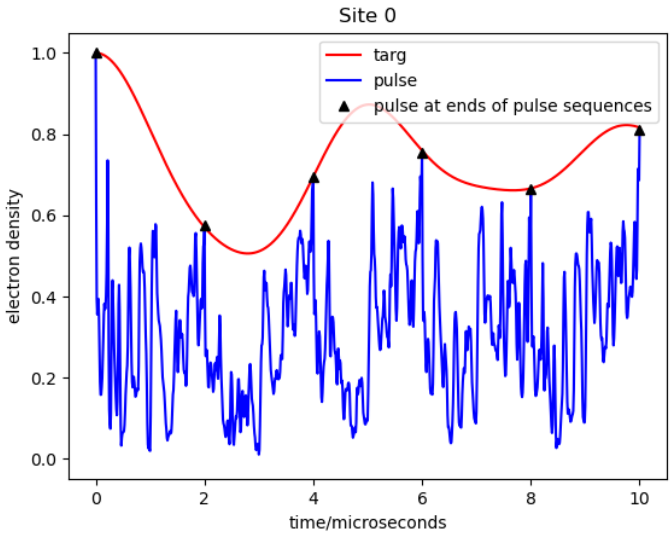

Figure 1: Example site electron densities with site Hamiltonians. The pulse-driven dynamics are marked black at the end of each pulse sequence for clarity.

1 Further verification for variational method

As demonstrated before, when the variational method is used to calculate the ground state energy, it achieved a decent result with as small relative energy error as 1e-6. To verify and test the capability of the variational method, here presents some further results.

1.1 Behavior when close excited state is present

Here presents the case when hopping magnitude $J \approx 0.346$ and site energies $S_{1,2,3,4} = 0.00976$, 0.0430, 0.0206, 0.00898 respectively. All units in $\frac{1}{2\pi}$MHz. In this case, the ground state energy and first excited state energy are -0.6557 and -0.6448. The resulting variational algorithm result is shown in Figure 2. The comparison of relative energy error with respect to the ground state energy and firxt excited state energy is shown in Figure 3.

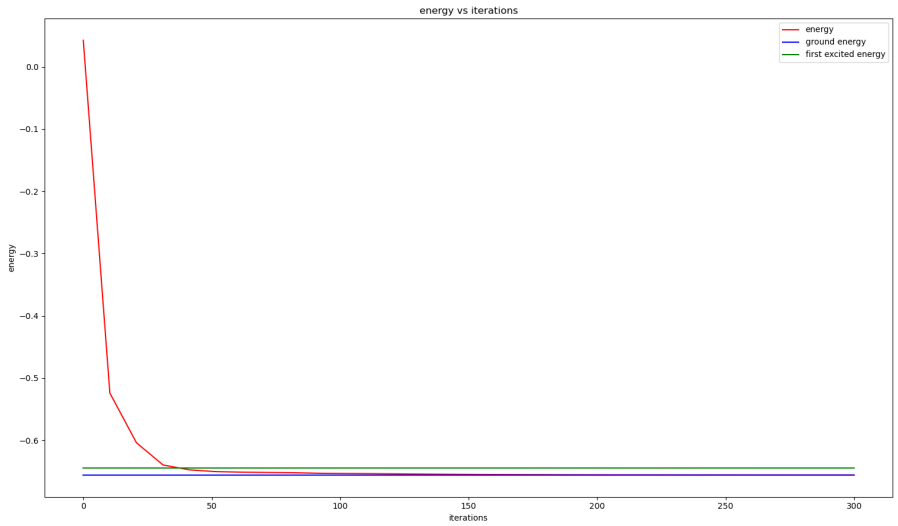

Figure 2: Energy of pulse-driven state. Ground state and excited state energies are lebelled.

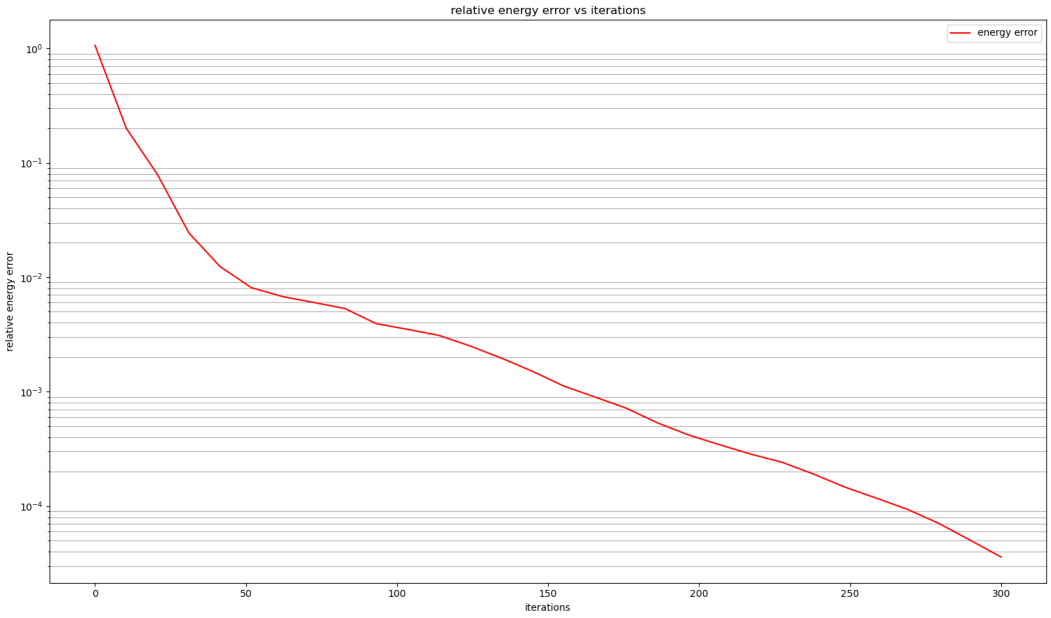

(a) Compared to ground state

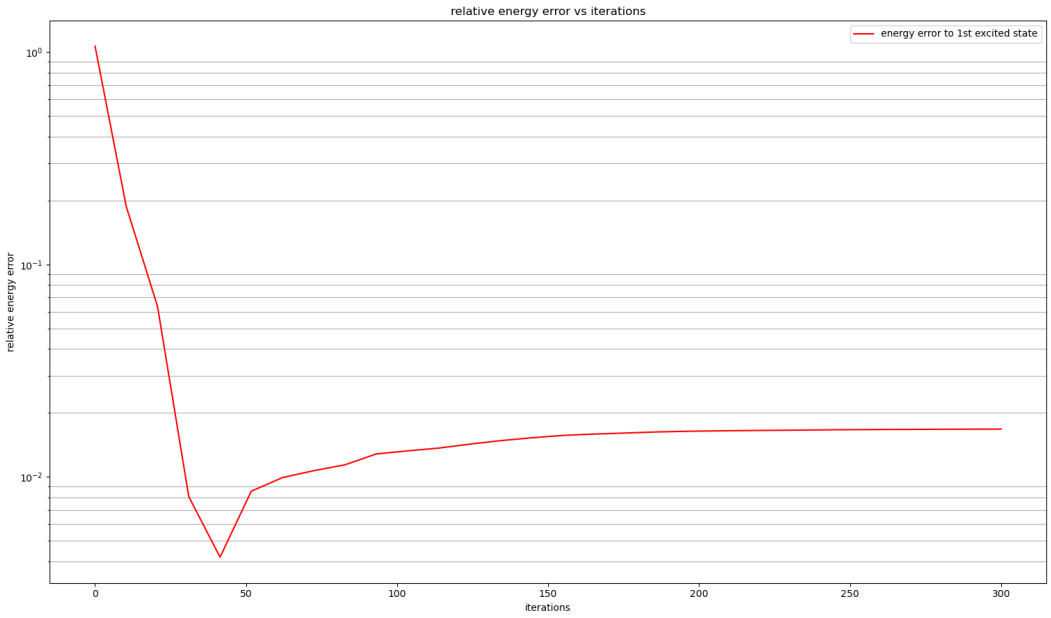

(b) Compared to first excited state

Figure 3: Semi-log plot of relative energy error vs number of iterations.

It can be seen that when the energy passes the first excited state energy, there is a change in gradient as expected. Overall, the algorithm is still working on approaching the ground state energy level.

1.2 Eigenstate projections

Let the eigenstates of the Hamiltonian be $|\psi_i\rangle$ sorted by energies such that $|\psi_0\rangle$ is the ground state. Here, the driven state $|\Psi\rangle$ is projected onto the eigenstates such that the values of $|\langle\Psi|\psi_i\rangle|$ are plotted in Figure 4. Worth noticing, the relative energy error in this case is on the same order as the error on ground state projection, i.e. relative energy error roughly 1e-6.

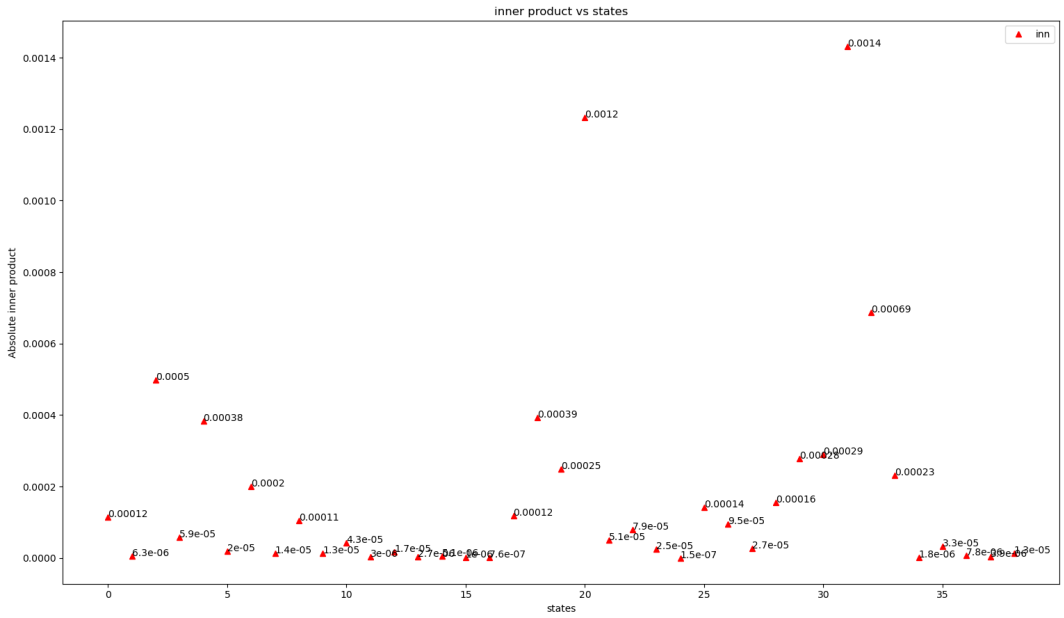

Figure 4: Eigenstate projection of driven state, excluding the ground state for clarity. The projection on ground state $|\langle\Psi|\psi_0\rangle| \approx 1 - 10^{-6}$

2 Tight-binding model generalization

Previously, only two spinless fermions are considered. Here, consider a broader case of spin 1/2 electrons. The Pauli exclusion principle only works for spin up electrons and spin down electrons respectively, i.e. spin up and spin down electrons can be regarded as distinguishable particles. Assume there are N_{site} number of sites, N_{up} spin up electrons, and N_{down} spin down electrons. In that case, the Hilbert space dimension should be

$$\dim(H) = \dim(H_{up}) \times \dim(H_{down}) = \binom{N_{site}}{N_{up}} \times \binom{N_{site}}{N_{down}}.$$

Therefore, the Hilbert space dimension is biggest when the number of spin up/down electrons are at about half the number of sites. 3D plots are shown in Figure 5 for N_{site} equal to 4 and 8. When $N_{site} = 8$, the maximum case of $N_{up} = N_{up} = 4$ gives a Hilbert space dimension of 4900.

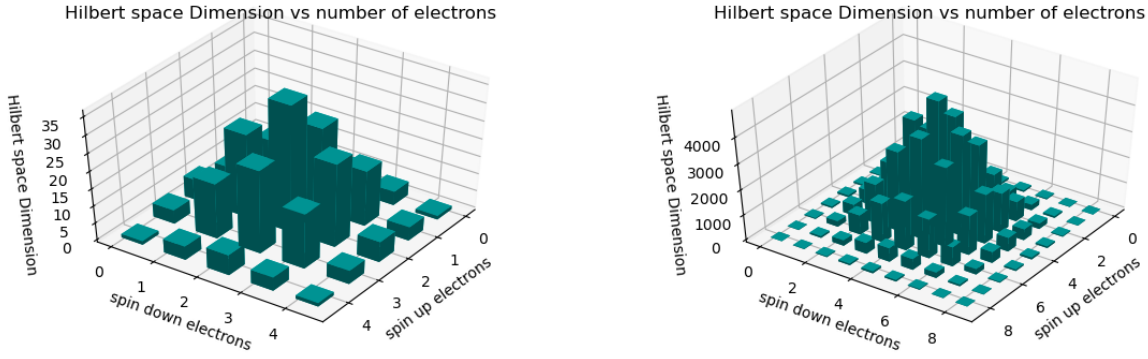

(a) $N_{site} = 4$ (b) $N_{site} = 8$

Figure 5: Hilbert space dimensions vs number of spin up/down electrons.

3 Tight-binding model: 2 spin-half electrons on 4 sites

3.1 Model

The Hubbard model states

$$\hat{H} = \hat{H}_{hop} + \hat{H}_{NN} = -J \sum_{i,\sigma} \left(\hat{c}^{\dagger}_{i,\sigma} \hat{c}_{i+1,\sigma} + \hat{c}^{\dagger}_{i+1,\sigma} \hat{c}_{i,\sigma} \right) + U \sum_{i} \hat{n}_{i,\uparrow} \hat{n}_{i,\downarrow},$$

where σ sums over up and down spins. As calculated before, the hopping Hamiltonian part for 1 and 2 spinless fermions on 4 sites are

$$\hat{H}_{1e} = -J \begin{pmatrix} 0 & 1 & 0 & 1 \\ 1 & 0 & 1 & 0 \\ 0 & 1 & 0 & 1 \\ 1 & 0 & 1 & 0 \end{pmatrix}.$$

Let the state of system be defined by $|v_{\uparrow}\rangle \otimes |v_{\downarrow}\rangle = |v_{\uparrow} v_{\downarrow}\rangle$, where v represents the site the electron occupies. For 1 spin up and 1 spin down electrons hopping on 4 sites, the hopping Hamiltonian is then

$$\hat{H}_{hop} = \hat{H}_{1e} \otimes \hat{I} + \hat{I} \otimes \hat{H}_{1e},$$

where $\hat{I}$ is the identity operator. The nearest-neighbor interaction Hamiltonian in this case is

$$\hat{H}_{NN} = U \sum_{i} |i\rangle\langle i| \otimes |i\rangle\langle i| = U \sum_{i} |ii\rangle\langle ii|.$$

If site energies are added, then

$$\hat{H}_{site} = \sum_{i,j} \left(S_i + S_j \right) |i\rangle\langle i| \otimes |j\rangle\langle j| = \sum_{i,j} \left(S_i + S_j \right) |ij\rangle\langle ij|.$$

Note that H_{hop}, H_{NN}, and H_{site} can be expressed by matrices of size 16×16. It is encoded in the cavity similarly as before. For example, when using 40 energy levels of the cavity, the hopping Hamiltonian expressing in the cavity is

$$\hat{H}_{hop,cav} = \begin{bmatrix} \hat{H}_{hop} & \\ & \hat{0} \end{bmatrix} \otimes |g\rangle\langle g|.$$

Here, $\hat{0}$ is a null matrix of size 24×24 and all other unlabelled elements are all zero as well. $\hat{P}_{gg} = |g\rangle\langle g|$ represents a projector on the qubit's ground state as usual.

The QuTip implementation is then modified accordingly such that it only concerns the first 16×16 element of the pulse-driven unitary.

Worth noticing that the unitary size expands a lot. Previously when dealing with the two spinless fermion case, only 6 energy levels were needed, so 20 energy levels were included to get rid of the margin effects, while 40 energy levels were used for the 2 spin-half fermion case. Therefore, the unitaries that are involved in the calculation expanded from 40×40 to 80×80.

3.2 Dynamics simulation results

Just to give an idea, set the parameters as usual such that $\chi = 2\pi \times 2.2\text{MHz}$, $J/\chi = 40$, and the evolution time $\tau = 2\mu\text{s}$. For simplicity, turn off nearest-neighbor interaction and site Hamiltonian. When the fidelity reaches 98.2%, the first 16×16 elements of the target unitary and the pulse driven unitaries are shown in Figure 6.

```
[[0.352 0.292 0.241 0.292 0.292 0.241 0.2   0.241 0.241 0.2   0.165 0.2   0.292 0.241 0.2   0.241]
 [0.292 0.352 0.292 0.241 0.241 0.292 0.241 0.2   0.2   0.241 0.2   0.165 0.241 0.292 0.241 0.2  ]
 [0.241 0.292 0.352 0.292 0.2   0.241 0.292 0.241 0.165 0.2   0.241 0.2   0.2   0.241 0.292 0.241]
 [0.292 0.241 0.292 0.352 0.241 0.2   0.241 0.292 0.2   0.165 0.2   0.241 0.241 0.2   0.241 0.292]
 [0.292 0.241 0.2   0.241 0.352 0.292 0.241 0.292 0.292 0.241 0.2   0.241 0.241 0.2   0.165 0.2  ]
 [0.241 0.292 0.241 0.2   0.292 0.352 0.292 0.241 0.241 0.292 0.241 0.2   0.2   0.241 0.2   0.165]
 [0.2   0.241 0.292 0.241 0.241 0.292 0.352 0.292 0.2   0.241 0.292 0.241 0.165 0.2   0.241 0.2  ]
 [0.241 0.2   0.241 0.292 0.292 0.241 0.292 0.352 0.241 0.2   0.241 0.292 0.2   0.165 0.2   0.241]
 [0.241 0.2   0.165 0.2   0.292 0.241 0.2   0.241 0.352 0.292 0.241 0.292 0.292 0.241 0.2   0.241]
 [0.2   0.241 0.2   0.165 0.241 0.292 0.241 0.2   0.292 0.352 0.292 0.241 0.241 0.292 0.241 0.2  ]
 [0.165 0.2   0.241 0.2   0.2   0.241 0.292 0.241 0.241 0.292 0.352 0.292 0.2   0.241 0.292 0.241]
 [0.2   0.165 0.2   0.241 0.241 0.2   0.241 0.292 0.292 0.241 0.292 0.352 0.241 0.2   0.241 0.292]
 [0.292 0.241 0.2   0.241 0.241 0.2   0.165 0.2   0.292 0.241 0.2   0.241 0.352 0.292 0.241 0.292]
 [0.241 0.292 0.241 0.2   0.2   0.241 0.2   0.165 0.241 0.292 0.241 0.2   0.292 0.352 0.292 0.241]
 [0.2   0.241 0.292 0.241 0.165 0.2   0.241 0.2   0.2   0.241 0.292 0.241 0.241 0.292 0.352 0.292]
 [0.241 0.2   0.241 0.292 0.2   0.165 0.2   0.241 0.241 0.2   0.241 0.292 0.292 0.241 0.292 0.352]]
```

(a) Target unitary

```
[[0.35  0.301 0.243 0.295 0.295 0.238 0.196 0.25  0.246 0.181 0.168 0.187 0.266 0.226 0.203 0.226]
 [0.305 0.35  0.286 0.26  0.241 0.295 0.237 0.202 0.189 0.226 0.181 0.168 0.225 0.288 0.245 0.157]
 [0.241 0.293 0.366 0.299 0.218 0.239 0.293 0.24  0.151 0.198 0.217 0.197 0.175 0.231 0.269 0.227]
 [0.303 0.246 0.291 0.37  0.257 0.209 0.248 0.307 0.18  0.159 0.185 0.231 0.21  0.183 0.235 0.238]
 [0.295 0.247 0.204 0.251 0.337 0.291 0.238 0.277 0.286 0.236 0.195 0.258 0.227 0.193 0.157 0.181]
 [0.237 0.301 0.237 0.208 0.29  0.343 0.298 0.246 0.223 0.302 0.237 0.197 0.21  0.22  0.171 0.165]
 [0.212 0.244 0.295 0.228 0.228 0.292 0.345 0.28  0.209 0.252 0.294 0.242 0.152 0.182 0.233 0.198]
 [0.256 0.209 0.249 0.301 0.288 0.227 0.282 0.335 0.241 0.204 0.259 0.281 0.198 0.151 0.17  0.237]
 [0.239 0.193 0.153 0.191 0.291 0.233 0.203 0.242 0.345 0.297 0.259 0.276 0.305 0.212 0.176 0.245]
 [0.203 0.232 0.187 0.15  0.232 0.289 0.235 0.212 0.288 0.363 0.296 0.235 0.243 0.29  0.233 0.188]
 [0.156 0.217 0.218 0.183 0.203 0.242 0.296 0.25  0.231 0.286 0.365 0.292 0.181 0.24  0.268 0.23 ]
 [0.196 0.155 0.192 0.24  0.239 0.194 0.227 0.303 0.293 0.229 0.303 0.34  0.23  0.199 0.232 0.274]
 [0.274 0.238 0.18  0.232 0.22  0.219 0.168 0.193 0.299 0.217 0.162 0.243 0.374 0.293 0.248 0.287]
 [0.209 0.274 0.258 0.179 0.219 0.224 0.177 0.154 0.246 0.278 0.227 0.196 0.289 0.359 0.305 0.233]
 [0.2   0.213 0.273 0.217 0.147 0.201 0.237 0.164 0.196 0.232 0.255 0.235 0.255 0.295 0.36  0.318]
 [0.207 0.17  0.218 0.253 0.172 0.148 0.19  0.231 0.247 0.196 0.233 0.285 0.284 0.266 0.305 0.384]]
```

(b) Pulse driven unitary

Figure 6: Explicit comparisons of the target and driven unitaries

With the same parameters, the fidelity error versus the number of iterations is plotted in Figure 7

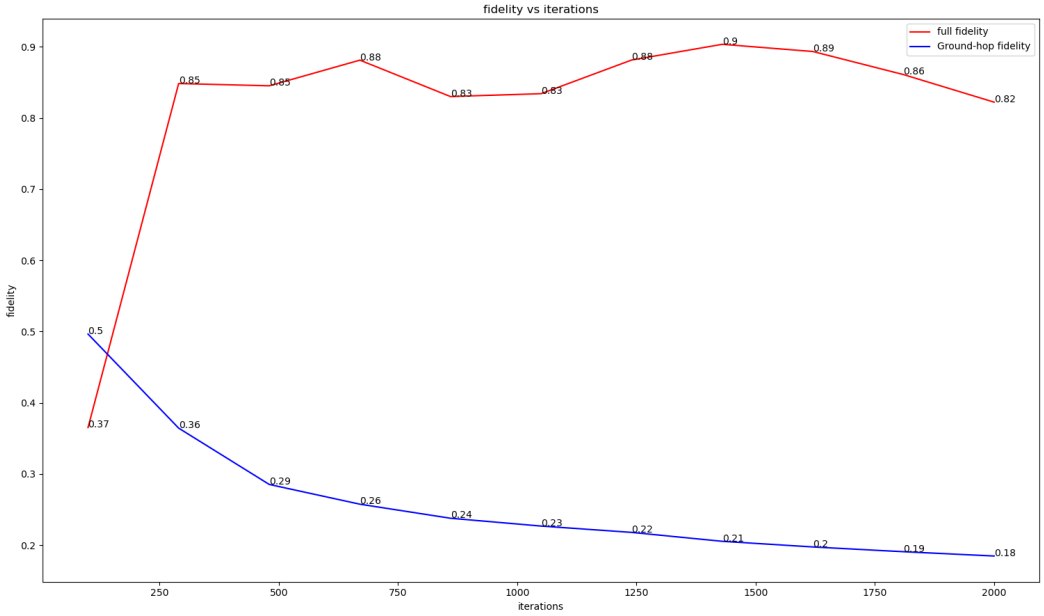

Figure 7: Fidelity error versus number of iterations. $J/\chi = 40$ and $\tau = 2\mu$s.

However, the fidelity error shown is still high. My guess is that the evolution time isn't long enough such that the control can reach all 16 levels. Therefore, in Figure 8 and 9, the product of $J \times \tau$ is kept constant, i.e. the target unitary is the same, but the J/χ ratio is increased to give the control more power. It can be seen that indeed when the ratio is increased, the fidelity error reached at 2000 iterations decreases, but still not reaching the same level as it did in the 2 spinless fermion case. Nevertheless, an increase of this ratio is rather not appreciated since when including the decoherence terms, the increase in evolution time τ brings trouble. Worth noticing, when simple decreasing the product $J \times \tau$, the fidelity error decreases, but that is simply the result from the target unitary approaching identity.

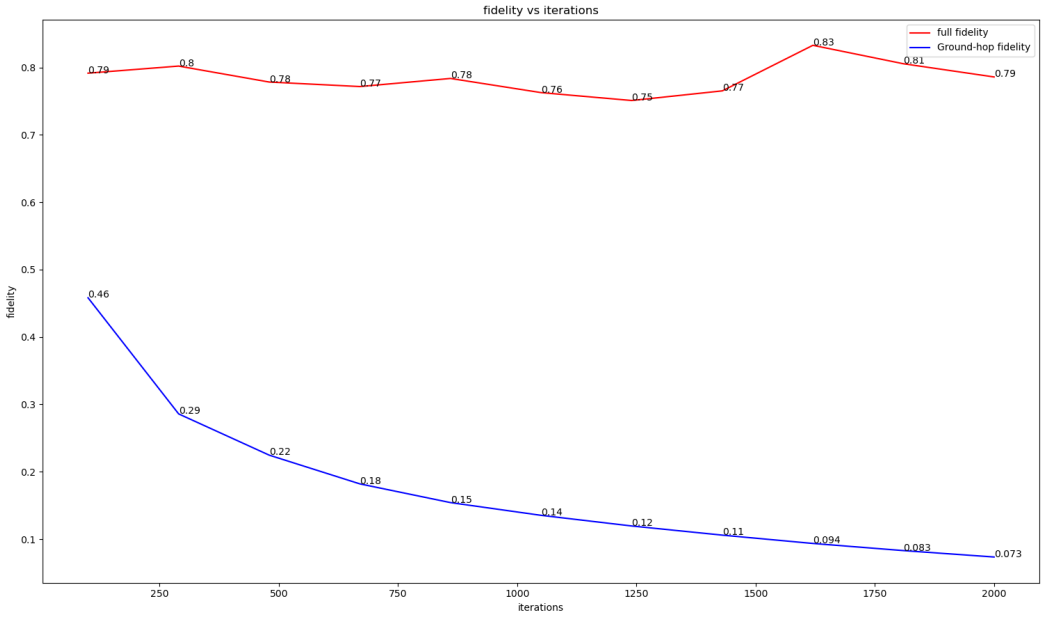

Figure 8: Fidelity error versus number of iterations. $J/\chi = 200$ and $\tau = 10\mu$s.

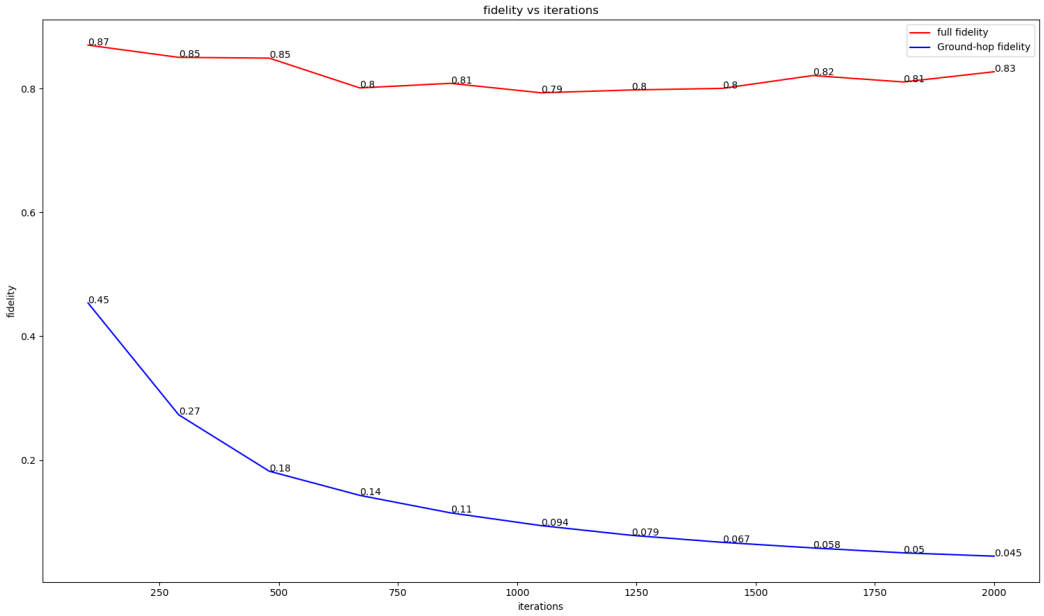

Figure 9: Fidelity error versus number of iterations. $J/\chi = 1000$ and $\tau = 50\mu$s.

3.3 Variational method results

While the dynamics simulation results aren't as good as before, variational method still works decently. The energy and relative energy error vs iteration are plotted in Figure 10 and 11.

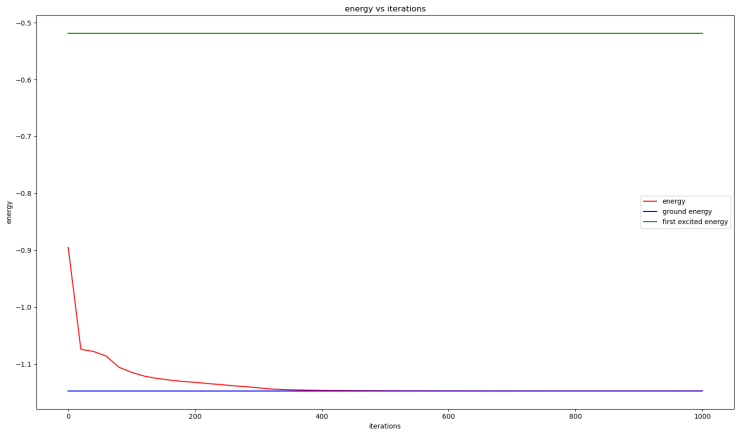

Figure 10: Energy of pulse-driven state. Ground state and excited state energies are lebelled.

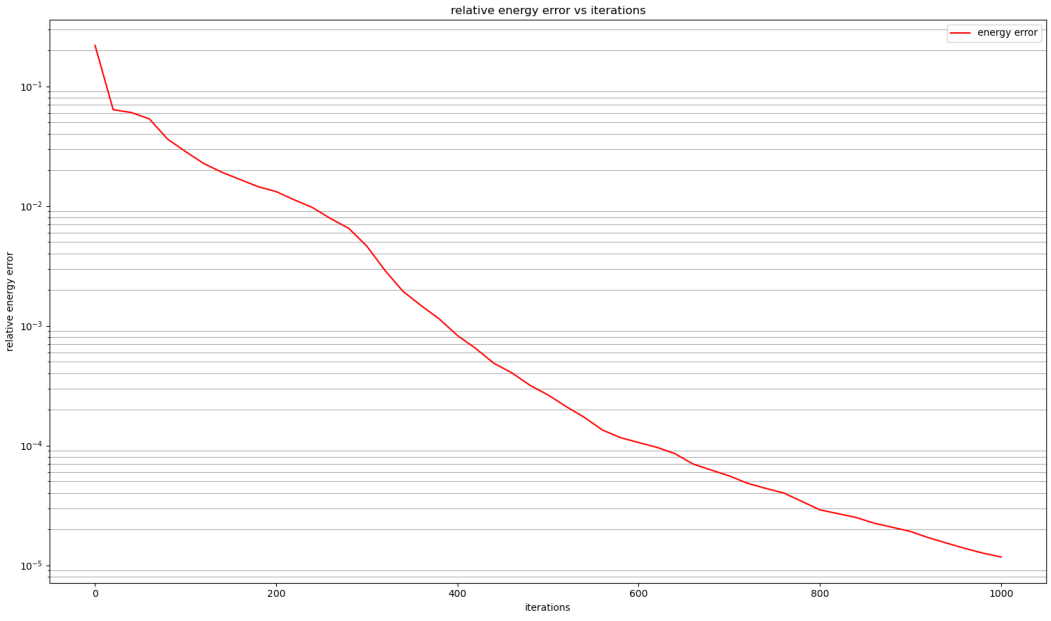

Figure 11: Semi-log plot of relative energy error vs number of iterations.

Although taking more iterations, the relative energy error still approaches the scale of 10^{-5}. This is expected, since variational method should be easier to achieve than dynamics simulation.

4 Control with double cavity

Here, encode the electron state $|v_\uparrow\rangle \otimes |v_\downarrow\rangle = |v_\uparrow v_\downarrow\rangle$ into the states of two cavities. Let the cavities and qubits be labelled to be 1 and 2, with states $|c_{1,2}\rangle$ and $|q_{1,2}\rangle$ respectively. The states in the cavity systems are defined to be $|c_1\rangle \otimes |q_1\rangle \otimes |c_2\rangle \otimes |q_2\rangle = |c_1 q_1 c_2 q_2\rangle$.

Since there are spin up and spin down electrons, they can correspond to the two cavities accordingly and be encoded one-to-one straightforwardly. This needs to define the Hamiltonians a bit differently than before. For example, let the number of energy levels in each cavity be 10. The hopping Hamiltonian of 1 spinless fermion in cavity is

$$\hat{H}_{1e,cavity} = -J \begin{pmatrix} \hat{H}_{1e} & \\ & \hat{0} \end{pmatrix},$$

where $\hat{0}$ is null matrix of size 6×6 and all other off-diagonal elements are zero as well. The hopping Hamiltonian of the two spin-half electrons are then

$$\hat{H}_{hop} = \hat{H}_{1e,cavity} \otimes \hat{P}_{gg} \otimes \hat{I}_{cav} \otimes \hat{P}_{gg} + \hat{I}_{cav} \otimes \hat{P}_{gg} \otimes \hat{H}_{1e,cavity} \otimes \hat{P}_{gg},$$

with $\hat{I}_{cav}$ the identity matrix of size 10×10. The site Hamiltonian and nearest-neighbor interaction Hamiltonian can be defined similarly.

Let the annihilation operators on the two cavities be $\hat{a}_1$ and $\hat{a}_2$, and the ones on the qubits be $\hat{\sigma}_1$ and $\hat{\sigma}_2$. The dispersive interaction Hamiltonian would then be

$$\hat{H}_{disp} = \chi \left(\hat{a}_1^\dagger \hat{a}_1 |e_1\rangle\langle e_1| + \hat{a}_2^\dagger \hat{a}_2 |e_2\rangle\langle e_2| \right).$$

The controls are then expanded to two sets, each acting on the two cavity-qubit systems,

$$\left\{ \hat{a}_1 + \hat{a}_1^\dagger, i\left(\hat{a}_1 - \hat{a}_1^\dagger\right), \sigma_{1,x}, \sigma_{1,y} \right\} \text{and} \left\{ \hat{a}_2 + \hat{a}_2^\dagger, i\left(\hat{a}_2 - \hat{a}_2^\dagger\right), \sigma_{2,x}, \sigma_{2,y} \right\}.$$

There is also the controls from the beam splitter that interacts between the two cavities

$$\left\{ \hat{a}_1^\dagger \hat{a}_2 + \hat{a}_1 \hat{a}_2^\dagger, i\left(\hat{a}_1^\dagger \hat{a}_2 - \hat{a}_1 \hat{a}_2^\dagger\right) \right\}.$$

The fidelity expression of QuTip also needs modification, i.e.

$$\text{fidelity} = \frac{Tr\left\{ \hat{I}'_{gg} \hat{U}_{targ}^{-1} \hat{U}_f \right\}}{N_{dim}},$$

where N_{dim} is the Hilbert space dimension of the dynamincs ($4 \times 4 = 16$ in this case). Define

$$\hat{I}'_{gg} = \hat{I}_{sites} \otimes |g\rangle\langle g| \otimes \hat{I}_{sites} \otimes |g\rangle\langle g|,$$

and

$$\hat{I}_{\text{sites}} = \sum_i^{\text{sites}} |i\rangle\langle i| = \begin{pmatrix} \hat{I} & \\ & \hat{0} \end{pmatrix},$$

where $\hat{I}$ is of size 4×4 and $\hat{0}$ is of size 6×6 as usual since there are 10 cavity energy levels used.

4.1 Results

Limited simulations has been done yet. By far the best result is increasing from initial fidelity of 0.0908 to final fidelity of 0.685 after 43 iterations. Although not verified, but my guess is that using double cavities might perform better than using only one. The reason is that when using two cavities, the effective number of level is only 4, which is much more accessible than previous case.

However, one problem is the time-consumption. The 43 iterations in this case took 4 hours to complete, which is far longer than before. The reasoning behind this can be:

1. The dimension of the unitary is much larger. For example, if set the parameters as I mentioned in the previous section, then the unitary is of size $10 \times 2 \times 10 \times 2 = 400$ when expressed in matrix form.

2. I have to switch to QuTip's built-in data type to perform tensor computation, while previously I am using numpy, another python library. This might slow down the process. I haven't looked into how numpy supports tensor product yet.